AJNR

# Whole-Brain *N*-Acetylaspartate Spectroscopy and Diffusion Tensor Imaging in Patients with Newly Diagnosed Gliomas: A Preliminary Study

M. Inglese, S. Brown, G. Johnson, M. Law, E. Knopp and O. Gonen



*AJNR Am J Neuroradiol* 2006, 27 (10) 2137-2140
http://www.ajnr.org/content/27/10/2137

ORIGINAL RESEARCH

# Whole-Brain *N*-Acetylaspartate Spectroscopy and Diffusion Tensor Imaging in Patients with Newly Diagnosed Gliomas: A Preliminary Study

M. Inglese
S. Brown
G. Johnson
M. Law
E. Knopp
O. Gonen

**BACKGROUND AND PURPOSE:** Glial cancer cells can be found well beyond the MR imaging T2 signal-intensity hyperintensity. To quantify the extent of the diffuse microstructural tissue damage possibly due to the presence of these satellite tumor cells, we investigated the relationships between global metabolic and microstructural abnormalities in the normal-appearing brain regions of patients with newly diagnosed glioma.

**MATERIAL AND METHODS:** Ten patients (6 men, 4 women) with radiologically suspected untreated supratentorial glial tumors and 9 healthy controls (5 men, 4 women) were studied with T1- and T2-weighted MR imaging, diffusion-weighted echo-planar MR imaging, and whole-brain *N*-acetylaspartate (WBNAA) proton MR spectroscopy. The relationship between the WBNAA concentration, the mean diffusivity (MD), and fractional anisotropy (FA) values in a large contralateral normal-appearing white matter (NAWM) brain region was investigated with the Spearman rank correlation test.

**RESULTS:** WBNAA values were significantly lower ($P < .001$) in patients (9.7 ± 1.7 mmol/L) than controls (13.1 ± 1.1 mmol/L). MD values were higher ($P = .0001$) in patients (0.95 ± 0.07 $mm^2s^{-1}$) than in controls (0.61 ± 0.04 $mm^2s^{-1}$). FA values did not differ between patients (0.42 ± 0.08) and controls (0.43 ± 0.041). A strong inverse correlation between WBNAA and MD ($r = -0.88$, $P = .0008$) was found in the patients but not in controls ($r = 0.012$, $P = .975$).

**CONCLUSION:** The correlation between the WBNAA and MD in the contralateral NAWM suggests that the microstructural damage possibly related to the presence of infiltrative tumor cells contributes to WBNAA decline in these patients.

Gliomas are the most common histologic subtype of primary brain tumors, ranging in malignancy from low grade (World Health Organization [WHO] grade I, II) to anaplastic (WHO grade III) and glioblastoma multiforme (WHO grade IV).[1-3] The higher grades, III and IV, affect approximately 10,000 new patients in the United States annually; and in addition to their physical morbidity and emotional challenges, their treatment costs may exceed $500,000 per patient.[2,3]

On conventional MR imaging, high-grade glial tumors appear as T2 signal intensity hyperintensities, indicating parenchyma infiltrated by tumor cells and edema with contrast-enhancing regions,[4] as shown in Fig 1. Glial tumors of various grades, however, are often invasive even beyond the T2 signal intensity abnormality, hindering surgical planning and precluding complete resection;[5] this probability accounts for the poor survival rates of patients with this disease.[6] Indeed, during surgery, distant satellite lesions can be found several centimeters from the original lesion.[7]

In the past, postmortem thin-section microscopic analysis was the only objective method of denoting infiltration as the cause of neuronal deficit.[8] Because this is not possible in newly diagnosed patients, whole-brain quantification of the amino acid derivative *N*-acetylaspartate (NAA), found exclusively in neuronal cells and their processes,[9,10] could be deployed as a surrogate for infiltrative damage. Most recently, Cohen et al[8] have shown preoperative patients with glioma to exhibit an average 26% lower whole-brain NAA (WBNAA) than matched controls, despite small tumor sizes averaging only 3% of the brain volume (ie, most of the NAA loss occurred outside the MR imaging–visible lesion).

Intracranial neoplasms frequently induce changes in both peritumoral and distal regions that affect the motion of interstitial water.[11,12] The changes in magnitude and directionality of this motion can be obtained with diffusion tensor imaging (DTI), which measures mean diffusivity (MD) and fractional anisotropy (FA).[13-15] Price et al[16] showed that infiltrated peritumoral white matter (WM) tracts in the brain have an increase in the isotropic MD and a less-marked reduction of the anisotropic FA components compared with analogous brain regions in healthy controls. This finding supports the hypothesis that in the early stages of invasion, glioma cells grow in interneuronal space, affecting first the isotropic diffusion (ie, DTI changes relate to glioma infiltration and cellularity).[16]

In a previous study of 17 patients with newly diagnosed gliomas, we observed a marked WBNAA decline compared with WBNAA of matched controls.[8] The hypothesis tested was that WBNAA decline reflected diffuse neuronal cell damage throughout the brain. Because the WBNAA method is nonlocalizing, however, that study left open 2 questions. First, was the observed NAA decline diffuse over the whole brain or restricted to 1 region (or a few regions) of severe loss? Second, did the decline indicate axonal loss or potentially reversible dysfunction?

In an attempt to resolve these issues, the present study aimed to retrospectively investigate the relationship between the WBNAA level and the DTI metrics in the normal-appearing WM (NAWM) contralateral to the MR imaging–visible

Received October 20, 2005; accepted after revision January 27, 2006.

From the Department of Radiology, New York University School of Medicine, NY.

This work was supported by NIH grants EB01015 and CA92547.

Please address correspondence to Oded Gonen, PhD, Department of Radiology, New York University School of Medicine, 650 First Ave, 6th Floor, New York, New York 10016; e-mail: oded.gonen@med.nyu.edu

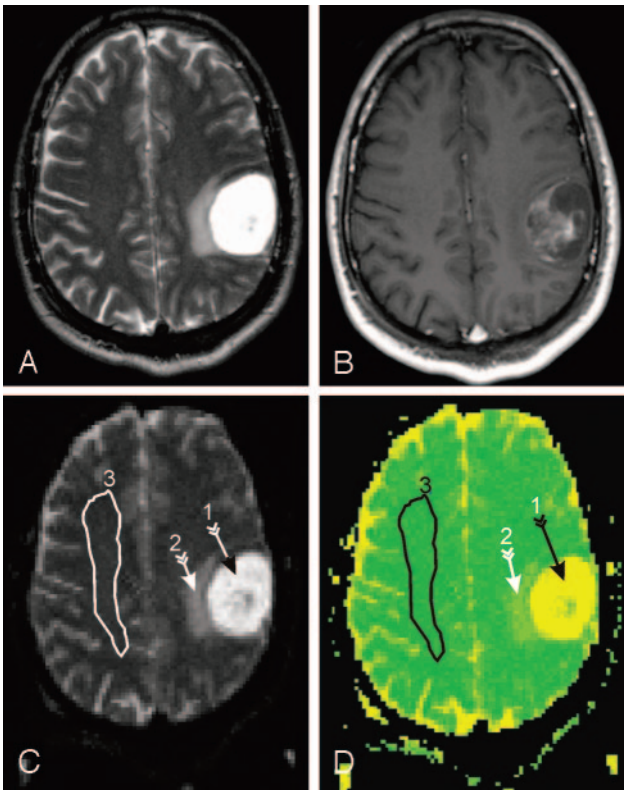


**Fig 1.** *A*, Top left, axial T2-weighted MR image of a section containing the lesion (mixed glioneurocytoma grade II) in patient 4 in the Table.

*B*, Top right, postcontrast T1-weighted image of the same section.

C, Bottom left, DTI ($b = 0$) image from the same level as *A* and *B* and the contralateral NAWM ROIs used for the MD and FA analyses 3.

*D*, Bottom right, color-coded MD map of the same section showing the marked elevated MD in the tumor and surrounding tissue, analogous to regions 1 and 2 in *C*. Note that the ROI selected does not contain any apparent tissue abnormalities.

tumor of these patients. The underlying hypothesis was that the decrease of WBNAA reported previously was not merely a reflection of the peritumoral neuroaxonal injury (the first question above). Rather, because of its severity, it might also reflect neuroaxonal injury distal to the lesion, related to/resulting from the presence of infiltrative tumor cells. If true, the WBNAA decrease should be related to the microscopic tissue damage reflected by MD and FA changes in the contralateral NAWM, addressing, in part, the second issue, mentioned previously.

## Materials and Methods

### *Human Subjects*

This retrospective study was approved by our institutional review board for ethics with no requirement for additional written consent. MR imaging data from 10 patients (6 men, 4 women; mean age, 43.6 years; range, 23–74) with radiologically suspected untreated supratentorial glial tumors, who underwent a preoperative MR imaging including DTI and WBNAA quantification before tumor resection, were analyzed retrospectively. Their age, sex, and histologic diagnosis are given in the Table. MR data from 9 healthy controls (5 men, 4 women; mean age, 35.1 years; range, 18–54), previously scanned by using the same protocol, were also used.

### *MR Imaging Segmentation: Volumetry*

All MR imaging measurements were obtained in a 1.5T Magnetom Vision scanner (Siemens, Erlangen, Germany) by using its standard head coil. All subjects' brain volumes, $V_B$, were obtained from T1-weighted sagittal magnetization-preparation rapid gradient-echo (TE/TR/TI, 7.0/14.7/300 ms; 128 sections 1.5 mm thick; 256 ×256 matrix; 210 × 210 mm$^2$ FOV) images by using the MIDAS package.[17] A "seed" region was placed in the periventricular WM. After all pixels at or above the gray matter (GM) signal intensity were selected, a brain mask was constructed in 3 steps: (1) morphologic erosion, (2) recursive region growth retaining pixels connected to the seed region; and (3) morphologic infiltration to reverse the effect of erosion. Brain masks were then truncated at the foramen magnum to incorporate the brain stem and cerebellum but not the cord. Finally, tumor beds that included pixels below GM intensity were incorporated in the presurgical masks, and $V_B$ was calculated from the mask, by multiplying the number of pixels in it by their volume.[8]

### *MR Spectroscopy: WBNAA Quantification*

Following shimming to a consistent 15 ± 4 Hz whole-head water line width, subjects' WBNAA signal intensity, $S_S$, was obtained with nonlocalizing nonecho (TE/TI/TR, 0/940/10 000 ms) $^1$H-MR spectroscopy.[18] Quantification was against a reference 3-L sphere of $1.5 \times 10^{-2}$ mol of NAA in water. $S_S$ and the reference peak, $S_R$, were integrated and the NAA amount of the brain, $Q_{NAA}$, scaled as,[19]

$$1) \qquad Q_{NAA} = 1.5 \times 10^{-2} \cdot \frac{S_S}{S_R} \cdot \frac{V_S^{180°}}{V_R^{180°}} \text{ mol}$$

$V_R^{180°}$ and $V_S^{180°}$ were the transmitter voltages into 50Ω for nonselective 1-ms 180° inversion pulses on the reference and subject, respectively, reflecting their relative coil loading.

We accounted for natural variations in head sizes by calculating the specific concentration,

$$2) \qquad \text{WBNAA} = \frac{Q_{NAA}}{V_B} \text{ mmol/L},$$

which is independent of brain size and, thus, suitable for cross-sectional comparison. Intra- and intersubject variability of WBNAA measurement was shown to be better than ±6%.[18] WBNAA values in this study were assessed by 2 readers, and the results were obtained by consensus.

### *DTI*

DTI was performed with a diffusion-weighted echo-planar imaging sequence: TE/TR, 98/4000 ms; 20 contiguous 5.0-mm-thick sections; 4 averages; 128 × 128 matrix; 240 × 240 mm$^2$ FOV; and 1-minute 44-second scanning time. Seven DTI image sets were acquired: 1 without diffusion-weighting and 6 with noncollinear weighting along gradient (Gx, Gy, Gz) directions (1, 1, 0), (0, 1, 1), (1, 0, 1), (−1, 1, 0), (0 , −1, 1), and (1, 0, −1), with a $b$ value of 1000 s/mm$^2$, in a dual-echo sequence optimized for minimal eddy currents and geometric distortion.[20] Raw data were processed off-line with an in-house program in the interactive data language (IDL, Research Systems Inc, Boulder, Colo).

MD and FA were calculated pixel by pixel by using the standard definitions,

$$3) \qquad \text{MD} = \bar{\lambda} = \frac{\lambda_1 + \lambda_2 + \lambda_3}{3}$$

**Patient information**

| Patient | Age (Years)/ Sex | Pathology | Tumor Resection Volume (mL) | WBNAA mmol/L | MD ($mm^2s^{-1}$) | Clinical Follow-up: Status, Time Elapsed Since Surgery |
|---|---|---|---|---|---|---|
| 1 | 55/M | Anaplastic Mixed GGNC (III) | 45 | 8.4 | 1.068 | Deceased, 6 months |
| 2 | 49/F | GBM (IV) | 59 | 9.5 | .940 | Deceased, 12 months |
| 3 | 35/M | GBM (IV) | 99 | 10.7 | .923 | Deceased, 12 months |
| 4 | 37/M | Mixed GN (II) | N/A | 8.6 | .953 | Stable, 17 months |
| 5 | 30/M | Mixed GN (II) | 9 | 9.2 | .982 | Stable, 15 months |
| 6 | 23/F | GGNC-DNT (I) | 32 | 12.6 | .894 | Stable, 10 months |
| 7 | 39/F | Mixed GN (II) | 37 | 12.2 | .917 | Stable, 12 months |
| 8 | 74/M | GBM (IV) | 75 | 7.8 | 1.065 | Deceased, 9 months |
| 9 | 62/M | Anaplastic GGNC (III) | 41 | 7.9 | 1.009 | Stable, 10 months |
| 10 | 32/F | Mixed GGNC (II) | N/A | 9.8 | .872 | Stable, 12 months |

**Note:**—WBNAA indicates whole-brain *N*-acetylaspartate; MD, mean diffusivity; GGNC, ganglioglioneurocytoma; DNT, dysembryoplastic neuroepithelial tumor; GN, glioneurocytoma; DFA, diffuse fibrillary astrocytoma; GBM, glioblastoma multiforme; N/A, below our measurement sensitivity of 9 $cm^3$.

$$4) \qquad FA = \sqrt{\frac{3}{2}} \cdot \sqrt{\frac{(\lambda_1 - \bar{\lambda})^2 + (\lambda_2 - \bar{\lambda})^2 + (\lambda_3 - \bar{\lambda})^2}{\lambda_1^2 + \lambda_2^2 + \lambda_3^2}},$$

where the λn are the eigenvalues of the diffusion tensor. After the MD and FA maps were calculated, a board-certified neuroradiologist and a neurologist, each with more than 5 years' experience, worked in consensus to identify a NAWM region of interest (ROI). Specifically, 1 representative section demonstrating the largest aspect of the tumor was selected for each patient. ROIs (as large as possible, at least 200 voxels) were then drawn in the normal WM contralateral to the tumor (Fig 1). No voxels were excluded in the analysis. MD and FA mean ± SD in the ROI were calculated for each subject.

### *Statistical Analyses*

WBNAA, MD, and FA values from the patients were compared with those of the controls by using an exact Mann-Whitney *U* test. The association of the DTI with its corresponding WBNAA values was evaluated through Spearman rank correlations and least squares regression, with the latter used to assess the differences in correlations between patients and controls. All statistical computations were carried out by using SAS Version 9.0 (SAS Institute Inc, Cary, NC) and results were declared statistically significant when associated with a 2-sided $P \leq .05$.

## Results

Patients' age, sex, pathology, WBNAA, MD, and clinical outcome are given in the Table. Half of the 10 patients had postoperative diagnoses of high-grade glioma, commensurate with the epidemiology of this disease.[1] WBNAA values were significantly different between patients (9.7 ± 1.7 mmol/L [mean ± SD]) and healthy controls (13.1 ± 1.1 mmol/L) as shown by an exact Mann-Whitney *U* test of variance ($P = .0003$). Comparison of calculated MD values of patients (0.95 ± 0.07 $mm^2s^{-1}$) and controls (0.61 ± 0.04 $mm^2s^{-1}$) in the exact Mann-Whitney *U* test revealed significant differences between the 2 groups ($P = .0001$). No significant difference was found between patients' FA values (0.42 ± 0.08) and those of the controls (0.43 ± 0.041).

Pairwise Spearman correlations analysis revealed a strong negative correlation ($r = -0.879$, $P = .0008$) between WBNAA and MD in the patients. No correlation existed between WBNAA and FA or between MD and FA in patients ($P > 0.26$). The controls' data produced a significant correlation between WBNAA and FA ($R = 0.72$, $P = .03$) but none between WBNAA and MD or MD and FA ($P > 0.22$). The correlation between patients' WBNAA and MD was compared with that between control WBNAA and MD by using regression, though this finding was not significant ($P = .058$), as shown in Fig 2.

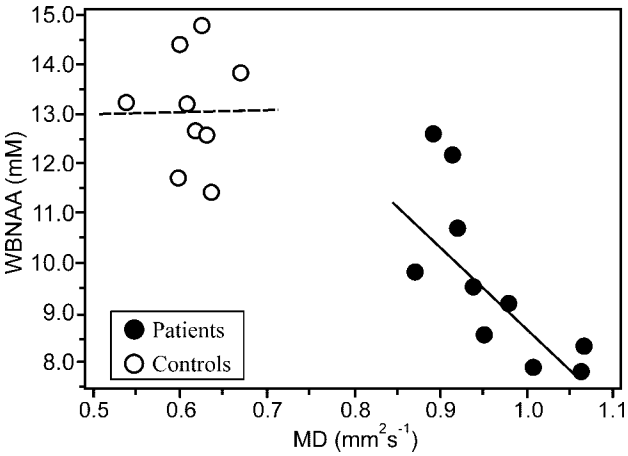


**Fig 2.** Scatterplot of WBNAA versus MD for the 10 patients (black circles) and 9 controls (white circles). The WBNAA deficit strongly inversely correlates with MD increase ($r = -0.879$, $P = .01$) in patients (WBNAA = −18.69.MD + 27.65, solid line) but not in controls ($r = 0.012$, $P = .975$, dashed line).

## Discussion

The mortality, morbidity, and cost implications of failing to distinguish low- from high-grade tumors or of failing to accurately identify the true extent of tumor infiltration are high. There is, therefore, a dire need for preoperative noninvasive comprehensive determination of tumor grade and extent for optimal treatment planning.[21] Because WBNAA provides a global measure of neuronal cell damage and might, therefore, reflect the total load of tumor infiltration (ie, be a surrogate marker for MR imaging–occult peripheral and distal infiltration). Because NAA decline can represent either neuronal dysfunction, which may be reversible, or a loss, it is necessary to distinguish these 2 possible mechanisms with an independent arbitrator. Absent gold standard pathology from the NAWM in these newly diagnosed patients, DTI may provide an alter-

native for this purpose because it is an accepted method of assessing microstructure disruption.[14-16]

Despite the specificity of NAA to neuronal cells, there are several possible mechanisms that could lead to potentially transient and, therefore, possibly reversible apparent decline. First, transient global edema, which increases the $V_B$ in the equation,[2] could be responsible, and its effect could be mitigated by, for example, debulking the primary tumor. Second, cytokines secreted by either the primary tumor or the proliferating cells may have a toxic effect on neurons, which would initially reduce their viability. Although this might ultimately lead to their death, in the earlier stages, this process might cause a recoverable decline. Third, reversible depression of neuronal-synaptic functions in areas of the central nervous system distal to an acute focal injury, diaschisis,[22] could lead to metabolic depression in regions that are distant from but anatomically linked to focal injury.

Because the MD is an accepted indicator of structural damage, its strong correlation with the WBNAA decline in our patients supports the hypothesis that NAA decrease is due not only to the peritumoral neuroaxonal injury but also to more-diffuse abnormalities distal to the tumor. Likewise, the significant difference between the MD in the NAWM contralateral to the tumor in the patients and the analogous region in the controls suggests the presence of infiltration, not only in the adjacent peritumoral zone but also many centimeters distal to the MR imaging–visible primary lesion as well, as shown in animal studies of high-grade astrocytomas by Geer and Grossman.[6]

The fact that despite a significant MD change (Fig 2), the FA values did not correlate with the WBNAA in the patients and also did not differ from those in the controls, as also observed previously by Price et al,[16] may suggest the nature of the invasive injury. Specifically, inspection of equations 3 and 4 defining the MD and FA show that a change of the former without the latter can only occur if the 3 axes of the diffusion spheroid inflate approximately proportionally. This could occur around tumor cells migrating along WM tracks and inducing local microedemas in their immediate vicinity.[6] These cells with their edematous penumbra would push the fibers apart along the short axes of the diffusion tensor but, at the same time, also extend the diffusion path along its long axis, increasing the magnitude of the diffusion path—the MD—but preserving, at least initially, its axes proportions—the FA.[16]

The main caveat of our study is the lack of pathologic correlates of WBNAA and DTI changes in the NAWM of patients with gliomas; experimental evidence is needed to prove neuronal loss rather than global edema, cytokine toxic effects, or depression of synaptic function. Although the sample size of our study was rather small, our findings suggest the potential role of WBNAA and DTI quantification as more comprehensive indicators of the pathologic processes underlying highly infiltrative tumors. Follow-up studies of WBNAA- and DTI-scanned patients should be conducted to determine the relationship between WBNAA levels on diagnosis and the most reliable of gold standard in this disease—survival. A larger patient cohort and longer follow-up may yield an even stronger correlation between these 2 variables. Further, larger scale assessment of relationships between WBNAA and MD, to localize the regions of greatest loss, should also take place to evaluate their joint potential for treatment planning (eg, deciding between focused, surgery, or focal radiation approaches versus more systemic chemo- or radiotherapy).

## References


1. Kleihues P, Soylemezoglu F, Schauble B, et al. **Histopathology, classification, and grading of gliomas** *Glia* 1995;15:211–21
2. DeAngelis LM. **Brain tumors.** *N Engl J Med* 2001;344:114–23
3. Surawicz TS, McCarthy BJ, Kupelian V, et al. **Descriptive epidemiology of primary brain and CNS tumors: results from the Central Brain Tumor Registry of the United States—1990–1994** *Neuro-oncol* 1999;1:14–25
4. Kelly PJ, Daumas-Duport C, Kispert DB, et al. **Imaging-based stereotaxic serial biopsies in untreated intracranial glial neoplasms.** *J Neurosurg* 1987;66:865–74
5. Lunsford LD, Martinez AJ, Latchaw RE. **Magnetic resonance imaging does not define tumor boundaries.** *Acta Radiol Suppl* 1986;369:154–56
6. Geer CP, Grossman SA. **Interstitial fluid flow along white matter tracts: a potentially important mechanism for the dissemination of primary brain tumors.** *J Neurooncol* 1997;32:193–201
7. Giese A, Bjerkvig R, Berens ME, et al. **Cost of migration: invasion of malignant gliomas and implications for treatment.** *J Clin Oncol* 2003;21:1624–36
8. Cohen BA, Knopp EA, Rusinek H, et al. **Assessing global invasion of newly diagnosed glial tumors with whole-brain proton MR spectroscopy.** *AJNR Am J Neuroradiol* 2005;26:2170–77
9. Simmons ML, Frondoza CG, Coyle JT. **Immunocytochemical localization of N-acetyl-aspartate with monoclonal antibodies.** *Neuroscience* 1991;45:37–45
10. Tsai G, Coyle JT. ***N*-acetylaspartate in neuropsychiatric disorders.** *Prog Neurobiol* 1995;46:531–40
11. Bitzer M, Nagele T, Geist-Barth B, et al. **Role of hydrodynamic processes in the pathogenesis of peritumoral brain edema in meningiomas.** *J Neurosurg* 2000; 93:594–604
12. Eis M, Els T, Hoehn-Berlage M, et al. **Quantitative diffusion MR imaging of cerebral tumor and edema.** *Acta Neurochir Suppl (Wien)* 1994;60:344–46
13. Lu S, Ahn D, Johnson G, et al. **Peritumoral diffusion tensor imaging of high-grade gliomas and metastatic brain tumors.** *AJNR Am J Neuroradiol* 2003;24: 937–41
14. Lu S, Ahn D, Johnson G, et al. **Diffusion-tensor MR imaging of intracranial neoplasia and associated peritumoral edema: introduction of the tumor infiltration index.** *Radiology* 2004;232:221–28
15. Oppenheim C, Rodrigo S, Poupon C, et al. **Diffusion tensor MR imaging of the brain: clinical applications** [in French]. *J Radiol* 2004;85:287–96
16. Price SJ, Pena A, Burnet NG, et al. **Tissue signature characterisation of diffusion tensor abnormalities in cerebral gliomas.** *Eur Radiol* 2004;14:1909–17; Epub 2004 Jun 25
17. De Santi S, de Leon MJ, Rusinek H, et al. **Hippocampal formation glucose metabolism and volume losses in MCI and AD.** *Neurobiol Aging* 2001;22: 529–39
18. Gonen O, Viswanathan AK, Catalaa I, et al. **Total brain N-acetylaspartate concentration in normal, age-grouped females: quantitation with non-echo proton NMR spectroscopy.** *Magn Reson Med* 1998;40:684–89
19. Soher BJ, van Zijl PC, Duyn JH, et al. **Quantitative proton MR spectroscopic imaging of the human brain.** *Magn Reson Med* 1996;35:356–63
20. Reese TG, Heid O, Weisskoff RM, et al. **Reduction of eddy-current-induced distortion in diffusion MRI using a twice-refocused spin echo.** *Magn Reson Med* 2003;49:177–82
21. Jansen EP, Dewit LG, van Herk M, et al. **Target volumes in radiotherapy for high-grade malignant glioma of the brain.** *Radiother Oncol* 2000;56:151–56
22. Bowler JV, Wade JP, Jones BE, et al. **Contribution of diaschisis to the clinical deficit in human cerebral infarction.** *Stroke* 1995;26:1000–06